Iraqi Journal of Science, 2024, Vol. 65, No.4, pp: 1999-2006
DOI: 10.24996/ijs.2024.65.4.18

ISSN: 0067-2904

Synthesis of Copper Oxide Nanostructures by Ar Plasma Jet and Study of Their Structural and Optical Properties

Bahaa Hassoun Abbas[1], Nisreen Kh Abdalameer[2], Raghad S. Mohammed[3,*]
1University of Sumer, College of Science, Thi-Qar, Iraq
2Department of Physics, College of Science for Women, University of Baghdad, Baghdad, Iraq
3Department of Physics, College of Science, Mustansiriyah University, Baghdad, Iraq

Received: 21/5/2022 Accepted: 25/4/2023 Published: 30/4/2024

Abstract

This paper used argon plasma jets to prepare CuO nanostructures. Several techniques, including UV–Vis spectroscopy, X-ray diffraction (XRD), X-ray energy dispersive spectroscopy (EDS), and scanning electron microscopy (SEM), were used for the characterization of the prepared CuO nanoparticles. UV–Vis spectroscopy analysis confirmed that the CuO nanostructures have an energy band gap of 2.7 eV. The XRD analysis showed that the CuO nanostructures have an average crystallite size of 36 nm. Furthermore, the results of the EDX examination demonstrated the creation of CuO nanostructures of high purity. The scanning electron microscope was used to analyze the surface morphology, showing a high agglomeration rate. According to SEM analysis, the average diameter of CuO nanoparticles was 10 nm.

Keywords: **P**lasma jets, Ar plasma, CuO nanostructures, Optical properties, Structural properties.

توليف تراكيب نانوية لأوكسيد النحاس بواسطة نفاثات بلازما الارجون ودراسة خصائصها التركيبية والبصرية

بهاء حسون عباس[1], نسرين خليل عبدالامير[2],رغد سعدون محمد[3,*]
[1] كلية العلوم, جامعة سومر, ذي قار, العراق
[2] قسم الفيزياء, كلية العلوم للبنات, جامعة بغداد, بغداد, العراق
[3] قسم الفيزياء, كلية العلوم, الجامعة المستنصرية, بغداد, العراق

الخلاصة

استخدت هذه الدراسة نفاثات بلازما الارجون لتصنيع تراكيب أوكسيد النحاس النانوية. تم استخدام العديد من التقنيات بما في ذلك التحليل الطيفي للأشعة فوق البنفسجية – المرئية، حيود الأشعة السينية (XRD)، التحليل الطيفي لتشتت طاقة للأشعة السينية (EDS)، والفحص المجهري الإلكتروني (SEM) لتوصيف تراكيب أوكسيد النحاس النانوية التي تم تصنيعها. أكد التحليل الطيفي للأشعة فوق البنفسجية – المرئية أن تراكيب أوكسيد النحاس النانوية لها فجوة طاقة تبلغ 2.7 الكترون فولت. يظهر تحليل الـ XRD أن تراكيب أوكسيد النحاس النانوية لها متوسط حجم بلوري 36 نانومتر. علاوة على ذلك، أظهرت نتائج فحص الـ EDS تخليق تراكيب أوكسيد النحاس النانوية عالية النقاوة. تم استخدام المجهر الإلكتروني الماسح لتحليل مورفولوجية السطح

*Email: raghad.almaliki@uomustansiriyah.edu.iq

والتي تمثل معدل تكتل عالي. كان معدل قطر تراكيب أوكسيد النحاس النانوية 10 نانومتر، وفقا لتحليل الـ SEM.

1. Introduction

In recent years, non-thermal plasma applications have developed significantly to include biomedical devices, biological materials, and material technologies [1]. The Atmospheric Pressure Plasma Jets (APPJs) are non-thermal plasmas with high electron and low gas temperatures. Using a gas flow creates a plasma plume with reactive species. Atmospheric Pressure Plasma Jets (APPJs) has achieved considerable advantage due to their favourable properties in industrial applications such as materials, electronics, and polymer processing potential [2-5]. The non-thermal plasma fabrication of metal nanostructures is a green alternative to chemical synthesis [6, 7]. Plasma provides significant advantages compared with other nanoparticle manufacturing technologies, including lower maintenance and operating expenses, shorter processing time, and no waste or harmful compounds [8]. Scientists and users are interested in metal oxide nanoparticles because their properties often differ from bulk materials [9]. The optical, electrical, magnetic, thermal, photoelectrochemical, mechanical, and catalytic properties make metal oxide nanoparticles widely used in various fields of application [10]. Copper oxide nanoparticles have unique physical and chemical properties and thus have attracted considerable attention as antibacterial materials, optoelectronic devices, solar cells, catalyst materials, lithium batteries, etc. [11].

This paper describes the synthesis of copper/copper oxide nanostructures via a plasma-water interaction, and studies some of their optical and structural properties.

2. Materials and Methods

As shown in Figure (1), the experimental setup for the fabrication of CuO nanostructures consisted of a high voltage DC power supply (20 kV), an argon gas cylinder, flowmeter, and two electrodes: a stainless steel tube as the cathode, and a copper foil (purchased from the british drug houses Ltd./london, Manufactured in England, 652247/470611) as the anode. The Cu foil was immersed in a glass beaker containing 5 ml of deionized water. Argon gas (99.99% purity) was utilized as the discharge gas, its flow was controlled with a flowmeter and fixed at 2 L/min. The plasma jet nozzle was around 2 cm away from the surface of the deionized water. The metal in the liquid was exposed to a plasma treatment for 1 min. The UV-Vis absorption spectra of the sample were recorded in the 200-900 nm wavelength range with a UV-Vis-NIR Metertech dual-beam spectrometer. The properties of the CuO nanoparticles were examined with an X-ray diffractometer (Phillips PANanaltical X'pert, Holland), SEM, and EDS techniques (TESCAN MIRA3, France), which were carried out in Iran at the University of Kashan.

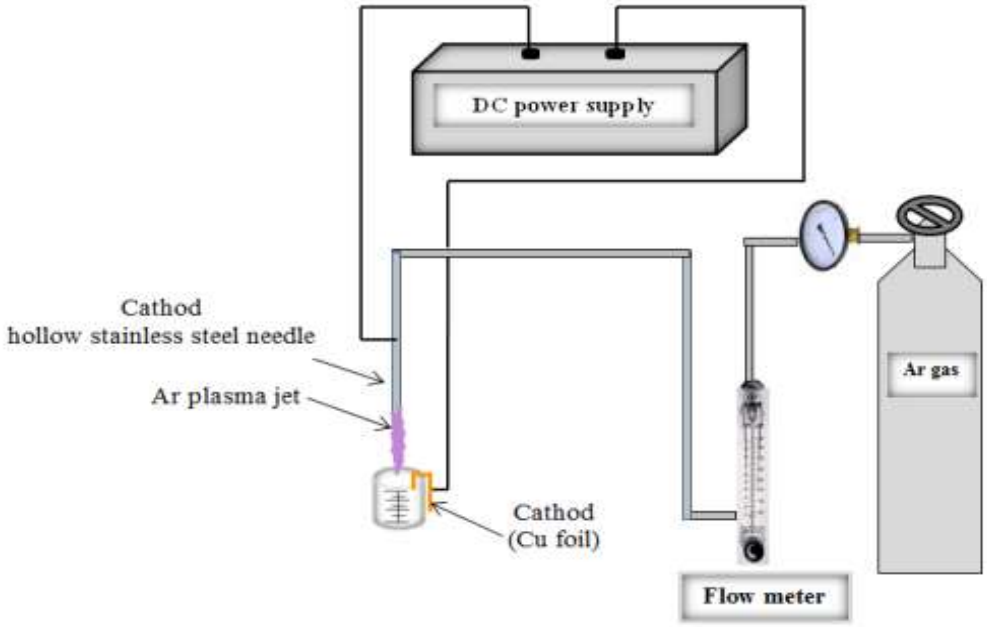

Figure 1: Schematic diagram of the plasma jet system to produce CuO nanoparticles.

3. Results and Discussion

3.1. Optical properties

The optical absorption properties of CuO nanostructures prepared with the argon atmospheric plasma jet (AAPJ) technology were studied using UV-Vis spectroscopy. Information regarding the nanoparticles' physical properties, such as their absorbance and bandgap energy, were obtained through optical characterization. The most important aspect of optical parameters is the band gap energy. Plotting the experimental absorbance data is a common procedure that is utilized in the process of determining the optical band gap energy of NPs. Planck's law, shown in Eq. (1) [7], was used to measure the bandgap energy directly from λ_{cut}:

$$E_g = \frac{hc}{\lambda} = \frac{1240}{\lambda} \quad \ldots\ldots (1)$$

Here Eg is the energy gap, h is Planck's constant=(6.626×10^{-34} J.s), c is the light velocity (3×10^8 m/s), and λ is the wavelength which can be determined by extrapolating the linear part of the absorbance spectrum.

In the UV-Vis absorption spectra of CuO nanostructures, a broad absorption peak was seen in the wavelength range 300 nm to 400 nm, as illustrated in Figure (2). The absorption edge shifted to longer wavelengths (red-shift), which decreased the optical band gap energy (E_g). A study by Mohammed et al. (2022) [7] suggests that the aggregation could have caused the red-shift in the samples.

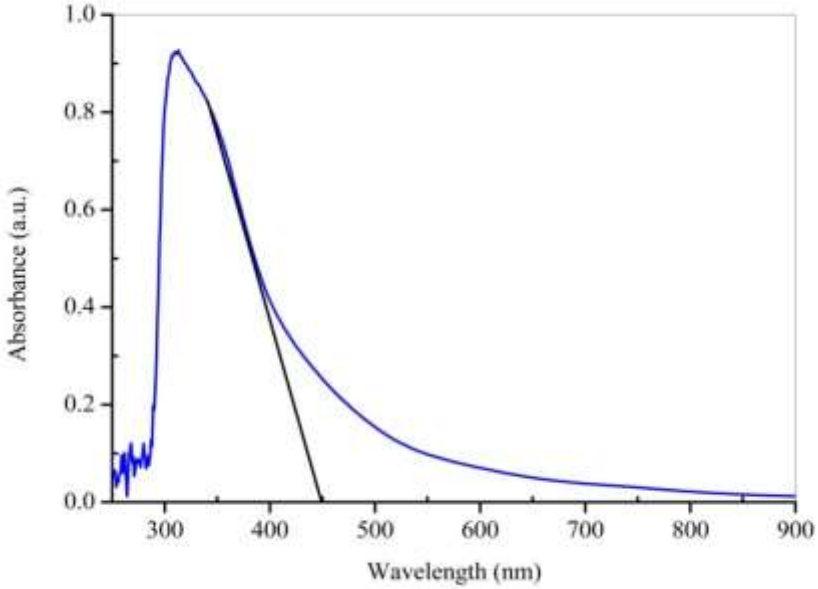

Figure 2: Optical absorption spectrum of CuO nanoparticles.

Using Tauc's relationship, Equation (2), for direct transition, the absorption coefficients of the CuO nanoparticles were calculated graphically [12]:

$$(\alpha h\upsilon)^r = A(h\upsilon - E_g) \ldots\ldots \quad (2)$$

The absorption coefficient is α, the photon frequency is υ, A is a constant equal to 0.9, the band gap energy is E_g, and r is a value of the direct transition (r = 2).

Figure (3) depicts a common approach for estimating a band gap energy by the intercept of the extrapolated linear part of the curve between the photon energy ($h\upsilon$) and $(\alpha h\upsilon)^r$ with the x-axis. The band gap energy was 2.7 eV, which is less than that reported in the literature [13, 14].

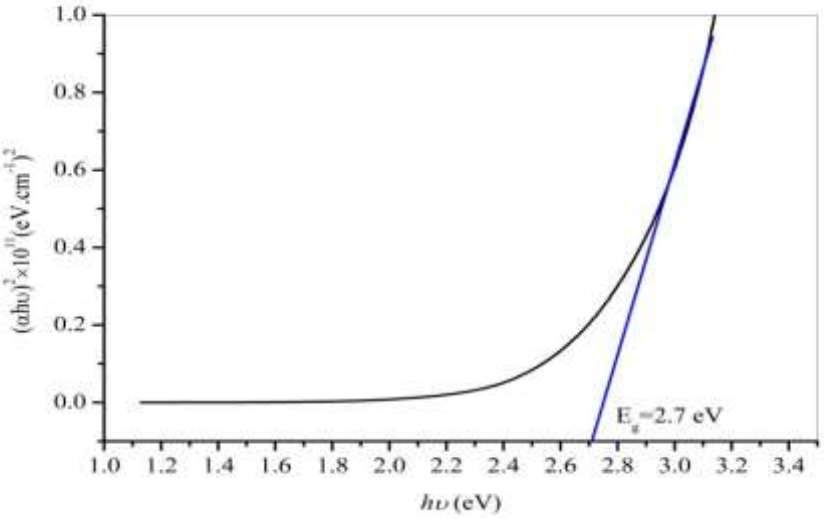

Figure 3: Band gap energy of CuO nanoparticles.

3.2. XRD analysis

According to the JCPDS card, the diffraction angles (2θ°) deducted from the XRD patterns confirmed the crystal structure and phase purity of the nanoparticles prepared by the argon atmospheric plasma jets (AAPJs) technique. As shown in Figure (4), the XRD pattern for the CuO nanostructures was recorded with a 2θ° diffraction angle between 15° to 70°. The broad diffraction peak at the diffraction angle of 25º suggests that the CuO nanoparticles are of an amorphous structure. The small peaks at diffraction angles of 18.3°, 24.4°, 33.6°, 38.2°, 43.54°, and 62.6° were associated with CuO crystal planes of (020), (021), (111), (427), (138), and (-113), respectively, related to the monoclinic crystal structure (JCPDS card No. 05-0661). There were no secondary peaks in the XRD pattern, indicating that the formed nanoparticles were pure.

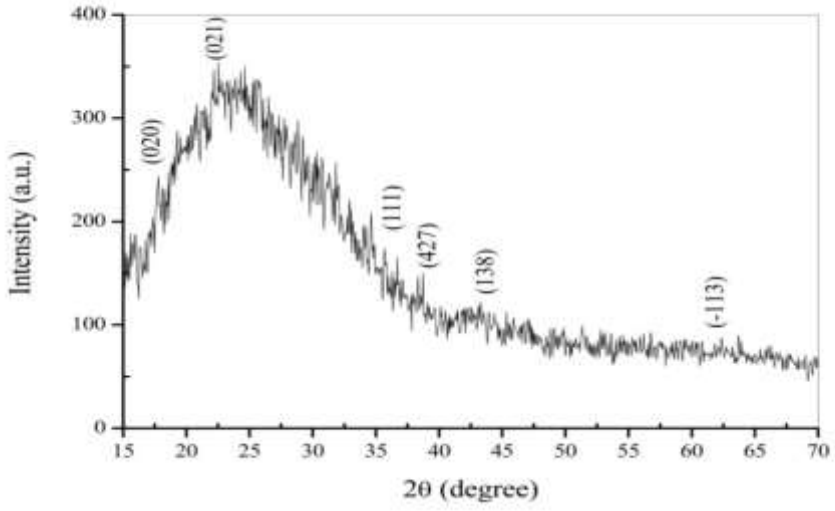

Figure 4: XRD pattern of CuO NPs generated by the plasma jet technique.

The crystallite size of the CuO NPs was calculated depending on Debye-Scherrer Equation (3) [15, 16]:

$$D\ (nm) = \frac{k\lambda}{\beta cos\theta} \ \ldots\ldots \quad (3)$$

Where: D is the crystallite size, k is a constant dependent on crystallite shape (0.94), λ is the X-ray wavelength (1.540 Å), and β is the full width at half maximum (FWHM) of the peaks at the θ diffraction angle from the Bragg's angle position. The average crystalline size of the CuO NPs was calculated to be equal to 36 nm.

3.3. SEM analyses

Scanning Electron Microscopy (SEM) photographs were used to analyze the morphologies of the CuO nanoparticles produced by the plasma jets method. The results of the SEM analysis showed that the particles prepared had the nature and morphology of nanoparticles, that the nanoparticles agglomerated, and that total separation was not obtained. According to the SEM image, the CuO NPs showed high agglomeration rate, as shown in Figure (5) the aggregation of the NPs can be attributed to some large size grains which are due to the increased surface area and surface energy of the CuO NPs. Because of the increased ratio of surface area to

volume, the nanoparticles were able to agglomerate or adhere together due to the attractive physical forces that existed between them [7]. "Image J" program was used to determine particle size from the SEM image analysis. Figure (6) shows that the average CuO nanoparticle diameter was 10 nm.

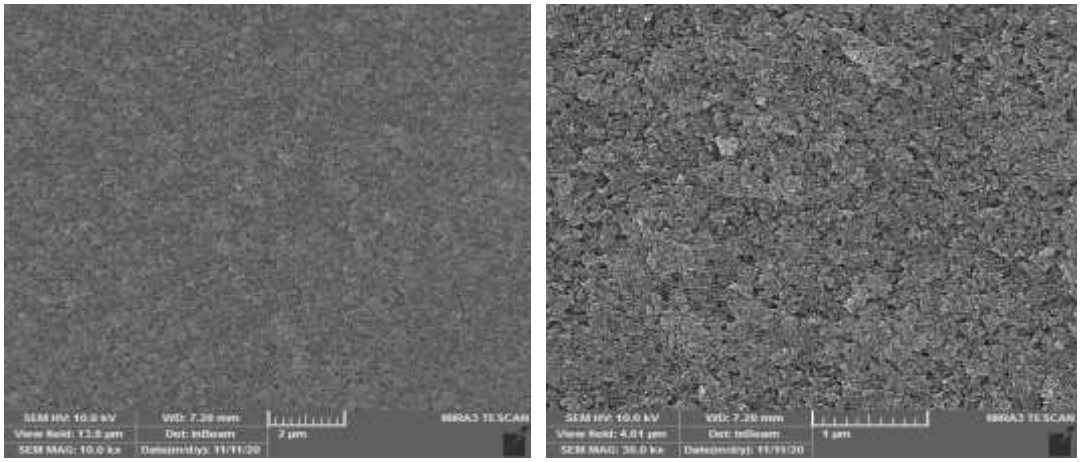

Figure 5: SEM images with different magnifications for CuO NPs generated by the plasma jet technique.

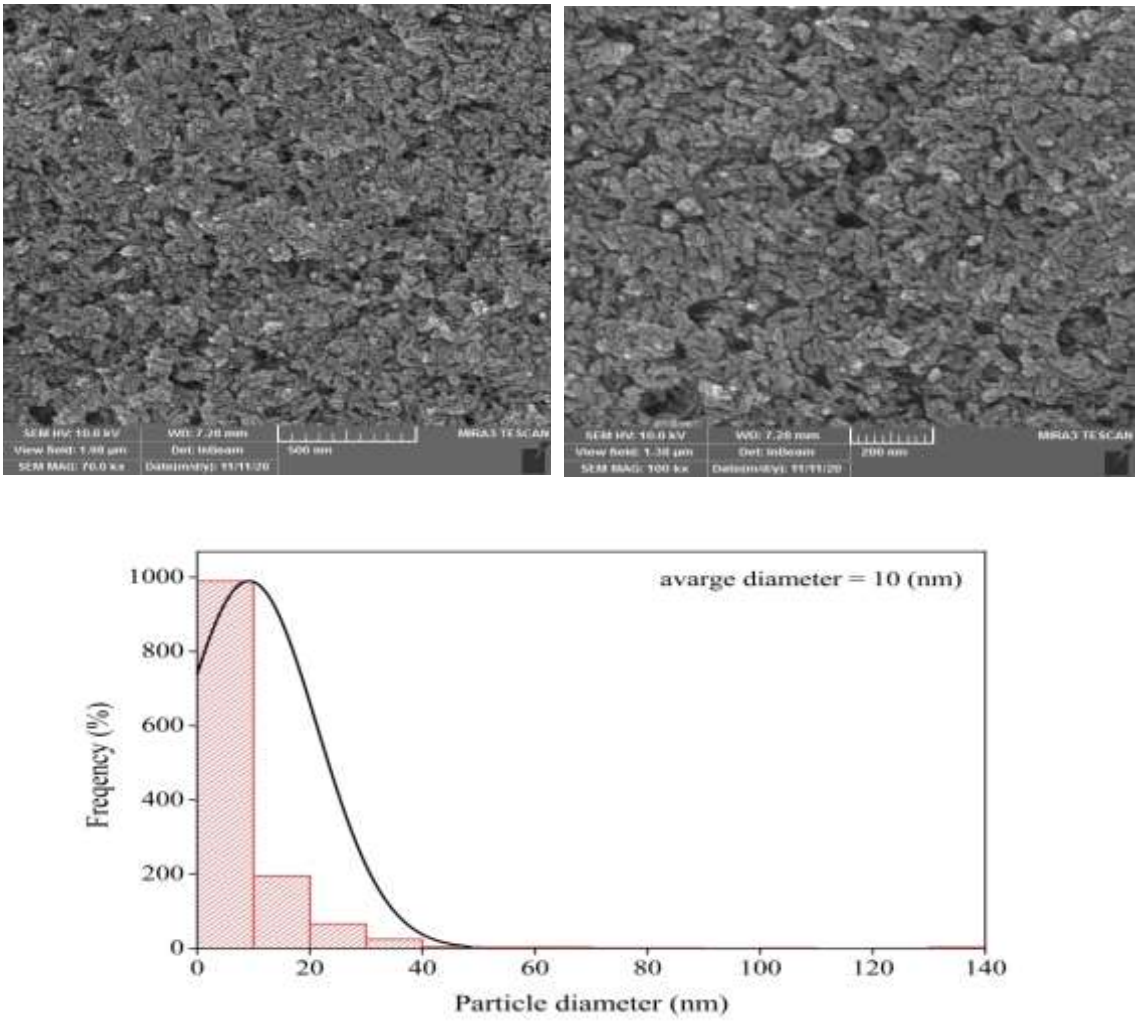

Figure 6: Diameter of particles histogram for CuO NPs generated by the plasma jet technique.

3.4. EDS analyses

Energy Dispersive X-ray Spectroscopy (EDX) analysis determined the chemical composition of the prepared CuO nanoparticles. Figure (7) shows the EDS spectrum of the CuO nanoparticles, which shows the existence of peaks associated with Cu and O elements. According to the results of the EDS examination, the composition of the CuO NPs was pure and free of impurity components. The Cu and O composition percentages (weight % and atomic %) in the CuO NPs are listed in Figure (7).

Element	Weight %	Atomic %
Cu	35.25	12.05
O	64.75	87.95
Total	100.00	100.00

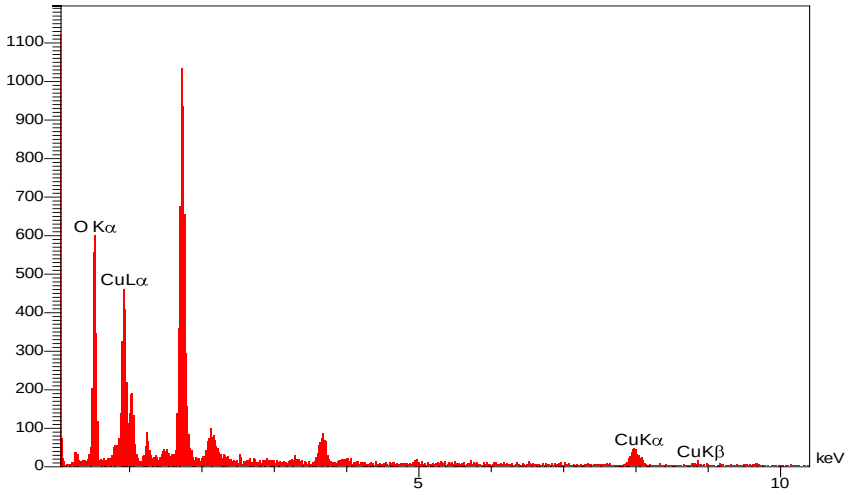

Figure 7: EDS spectrum for the CuO NPs generated by the plasma jet technique.

4. Conclusion

Copper oxide nanoparticles were successfully prepared using the argon plasma jet technique. Our work showed that CuO NPs had good absorption and bandgap properties and could be more active in visible light for photovoltaics. The nanoparticles were purely crystalline, with an average crystallite size of 36 nm, as confirmed by the XRD analysis. According to the findings of the SEM analysis, small aggregated particles with a mean diameter of 10 nm were observed. The EDS examination revealed that the CuO NPs had a pure composition, with no other impurity components.

Acknowledgements

We thank Plasma Physics Lab., Physics Department, College of Science, the University of Baghdad for supporting this work.

References

[1] R. S. Mohammed, K. A. Aadim, Kh. A. Ahmed, " Estimation of in vivo toxicity of MgO/ZnO core/shell nanoparticles synthesized by eco-friendly non-thermal plasma technology," *Applied Nanoscience*, vol. 12, pp. 3783–3795, 2022.

[2] F. Liu, B. Zhang, Z. Fang, M. Wan, H. Wan, K. Ostrikov, "Jet-to-jet interactions in atmospheric-pressure plasma jet arrays for surface processing," *Plasma processes and polymers*, vol. 15, no. 1, pp. 1-11, 2017 .

[3] S. Yatom, Y. Luo, Q. Xiong, P. J. Bruggeman, "Nanosecond pulsed humid Ar plasma jet in air: shielding, discharge characteristics and atomic hydrogen production," *Applied Physics D*, vol. 50, p. 415204, 2017.

[4] A. Segat, N. N. Misra, P. J. Cullen, N. Innocente, " Effect of atmospheric pressure cold plasma (ACP) on activity and structure of alkaline phosphatase," *Food and Bioproducts Processing*, vol. 98, pp. 181-188, 2016.

[5] M. A. Lietz, X. Damany, E. Robert, J. M. Pouvesle, M. J. Kushner." Ionization Wave Propagation in an Atmospheric Pressure Plasma Multi-jet," *Plasma Sources Science and Technology*, vol. 28, pp. 1-57, 2019.

[6] J. L. N. Nguyen, P. Lamichhane, E. H. Choi and G. J. Lee, " Structural and Optical Sensing Properties of Nonthermal Atmospheric Plasma-Synthesized Polyethylene Glycol-Functionalized Gold Nanoparticles," *Nanomaterials*, vol. 11, p. 1678, 2021.

[7] R. S. Mohammed, K. A. Aadim, Kh. A. Ahmed, " Synthesis of CuO/ZnO and MgO/ZnO Core/Shell Nanoparticles with Plasma Jets and Study of their Structural and Optical Properties," *Karbala International Journal of Modern Science*, vol. 8, pp. 213-222, 2022.

[8] T H. H. Murbat, N. KH. Abdalameer, A. Kh. Brrd, and F. abdulameer, " Effects of Non-Thermal Argon Plasma Produced at Atmospheric Pressure on the Optical Properties of CdO Thin Films," *Baghdad Science Journal*, vol. 15, no. 2, pp. 221- 226, 2018.

[9] G. Primc, K. Brenˇciˇc, M. Mozetiˇ, and M. Gorjanc, " Recent Advances in the Plasma-Assisted Synthesis of Zinc Oxide Nanoparticles," *Nanomaterials*, vol. 11, p. 1191, 2021.

[10] A. Hamdan, M. Agati, and S. Boninelli, "Selective Synthesis of 2D Mesoporous CuO Agglomerates by Pulsed Spark Discharge in Water," *Plasma Chemistry and Plasma Processing*, vol. 41, pp. 433–445, 2021.

[11] S. Sagadevan1, S. Vennila, A. R. Marlinda, Y. Al‑Douri, M. R. Johan, and J. A. Lett, "Synthesis and evaluation of the structural, optical, and antibacterial properties of copper oxide nanoparticles," *Applied Physics A*, vol. 125, p. 489, 2019.

[12] A. A. Menazea, "One-Pot Pulsed Laser Ablation route assisted copper oxide nanoparticles doped in PEO/PVP blend for the electrical conductivity enhancement," *Journal of Materials Research and Technology*, vol. 9, no. 2, pp. 2412–2422, 2020.

[13] A. A. Menazea and M. K. Ahmed, "Silver and copper oxide nanoparticles-decorated graphene oxide via pulsed laser ablation technique: Preparation, characterization, and photoactivated antibacterial activity," *Nano-Structures and Nano-Objects*, vol. 22, p. 100464, 2020.

[14] F. A. Hasan, M. T. Hussein, and M. A. Abdulsattar, " Structural, Optical,and Morphological Study of the Zinc Oxide Nano-Thin Films with Different Thickness Prepared by Pulsed Laser Deposition Technique, " *Iraqi Journal of Science*, vol. 63, no. 12, pp. 5242-5254, 2022.

[15] A. Ali, Y. Rammah, R. El-Mallawany, and D. Souri, " FTIR and UV spectra of pentaternary borate glasses, " *Measurement*, vol. 105, pp.72-77, 2017.

[16] A. J. Katafa and M. K. Hamid, " Influence of ZnO Nanoparticles on Candida albicansof Human Male Pleural Fluid, " *Iraqi Journal of Science*, vol. 61, no. 3, pp. 540-549, 2020.